Developmental Cell
Short Article

The Frizzled Extracellular Domain Is a Ligand for Van Gogh/Stbm during Nonautonomous Planar Cell Polarity Signaling

Jun Wu[1] and Marek Mlodzik[1,*]
[1]Mount Sinai School of Medicine, Department of Developmental and Regenerative Biology, 1 Gustav L. Levy Place, New York, NY 10029, USA
*Correspondence: marek.mlodzik@mssm.edu
DOI 10.1016/j.devcel.2008.08.004

SUMMARY

The Frizzled (Fz) receptor is required cell autonomously in Wnt/β-catenin and planar cell polarity (PCP) signaling. In addition to these requirements, Fz acts nonautonomously during PCP establishment: wild-type cells surrounding *fz*$^{-}$ patches reorient toward the *fz*$^{-}$ cells. The molecular mechanism(s) of nonautonomous Fz signaling are unknown. Our in vivo studies identify the extracellular domain (ECD) of Fz, in particular its CRD (cysteine rich domain), as critical for nonautonomous Fz-PCP activity. Importantly, we demonstrate biochemical and physical interactions between the FzECD and the transmembrane protein Van Gogh/Strabismus (Vang/Stbm). We show that this function precedes cell-autonomous interactions and visible asymmetric PCP factor localization. Our data suggest that Vang/Stbm can act as a FzECD receptor, allowing cells to sense Fz activity/levels of their neighbors. Thus, direct Fz-Vang/Stbm interactions represent an intriguing mechanism that may account for the global orientation of cells within the plane of their epithelial field.

INTRODUCTION

Frizzled (Fz) receptor signaling is required in both the Wnt/β-catenin pathway and planar cell polarity (PCP) establishment. In both pathways, Fz acts through the downstream effector Dishevelled (Dsh) (Boutros and Mlodzik, 1999; Mlodzik, 2002; Veeman et al., 2003; Wallingford and Habas, 2005). PCP is apparent in the precise organization of epithelial cells in many organs and tissues of both invertebrates and vertebrates (reviewed in Adler, 2002; Fanto and McNeill, 2004; Keller, 2002; Klein and Mlodzik, 2005; Lawrence et al., 2007; Montcouquiol et al., 2006; Seifert and Mlodzik, 2007; Tada, 2005; Wang and Nathans, 2007; Zallen, 2007). It has been most studied in *Drosophila*, where it is evident in the ordered arrangement of cells (or groups of cells) in, for example, the wing, abdomen, and eye (Adler, 2002; Klein and Mlodzik, 2005; Lawrence et al., 2007).

PCP establishment requires multiple steps of signaling activity, including a nonautonomous Fz signaling function (Adler, 2002; Klein and Mlodzik, 2005; Lawrence et al., 2007; Seifert and Mlodzik, 2007; Strutt and Strutt, 2002). The *Drosophila* wing is an excellent model system to study this aspect of PCP establishment, as each cell produces a single hair, which protrudes from the distal edge of the cell and extends further distally (see reviews above and Figure 1A). It was proposed that this distal orientation reflects a Fz activity slope (Adler, 2002; Adler et al., 1997), as cells commonly orient their distal surface toward regions of low Fz (activity) and their proximal surface toward high Fz (activity). This effect is often referred to as "domineering nonautonomy" (Vinson and Adler, 1987) and is apparent in most tissues in *Drosophila* (e.g., wing and abdomen [Casal et al., 2006; Lawrence et al., 2004; Vinson and Adler, 1987]) and also in mammals, including epidermal hair patterns in *mfz6* mutant chimeric mice (Guo et al., 2004), suggesting that nonautonomous Fz signaling is mediated by an evolutionarily conserved mechanism.

Only one other Fz group core PCP factor (distinct from the Fat-Dachsous PCP system) (Casal et al., 2006; Lawrence et al., 2007) also shows nonautonomous behavior: the multipass transmembrane factor *Van Gogh* (*Vang*, also known as *strabismus*/*stbm*; (Adler et al., 2000; Taylor et al., 1998; Wolff and Rubin, 1998). However, in contrast to *fz*, wild-type cells surrounding *Vang/stbm*$^{-}$ patches point away from the clone (Adler et al., 2000; Taylor et al., 1998). The relationship of the *fz* and *Vang/stbm* nonautonomous effects is not known, except that the defects associated with *fz*$^{-}$ clones are suppressed in *Vang/stbm*$^{-}$ backgrounds (Lawrence et al., 2004; Taylor et al., 1998) and that they depend on the presence of the atypical cadherin Flamingo (Fmi, also known as Starry Night/Stan) (Lawrence et al., 2004).

Here we address the role of Fz and Vang/Stbm in nonautonomous PCP signaling. We first show that the double mutant *fz*, *Vang/stbm* clones show a behavior that is very similar to *fz* single mutant clones, suggesting that Fz defines the direction of the nonautonomy. In vivo studies of different Fz isoforms indicate that the extracellular region (ECD), in particular the CRD (cystein rich domain) of Fz is required for its nonautonomous activity. We demonstrate molecular interactions between the Fz ECD (including the CRD) and the transmembrane protein Vang/Stbm. Our data suggest that Vang/Stbm can act as a Fz CRD receptor, allowing cells to sense the Fz activity/levels of their neighbors. We thus propose a mechanism underlying the global orientation of cells within the epithelial plane.

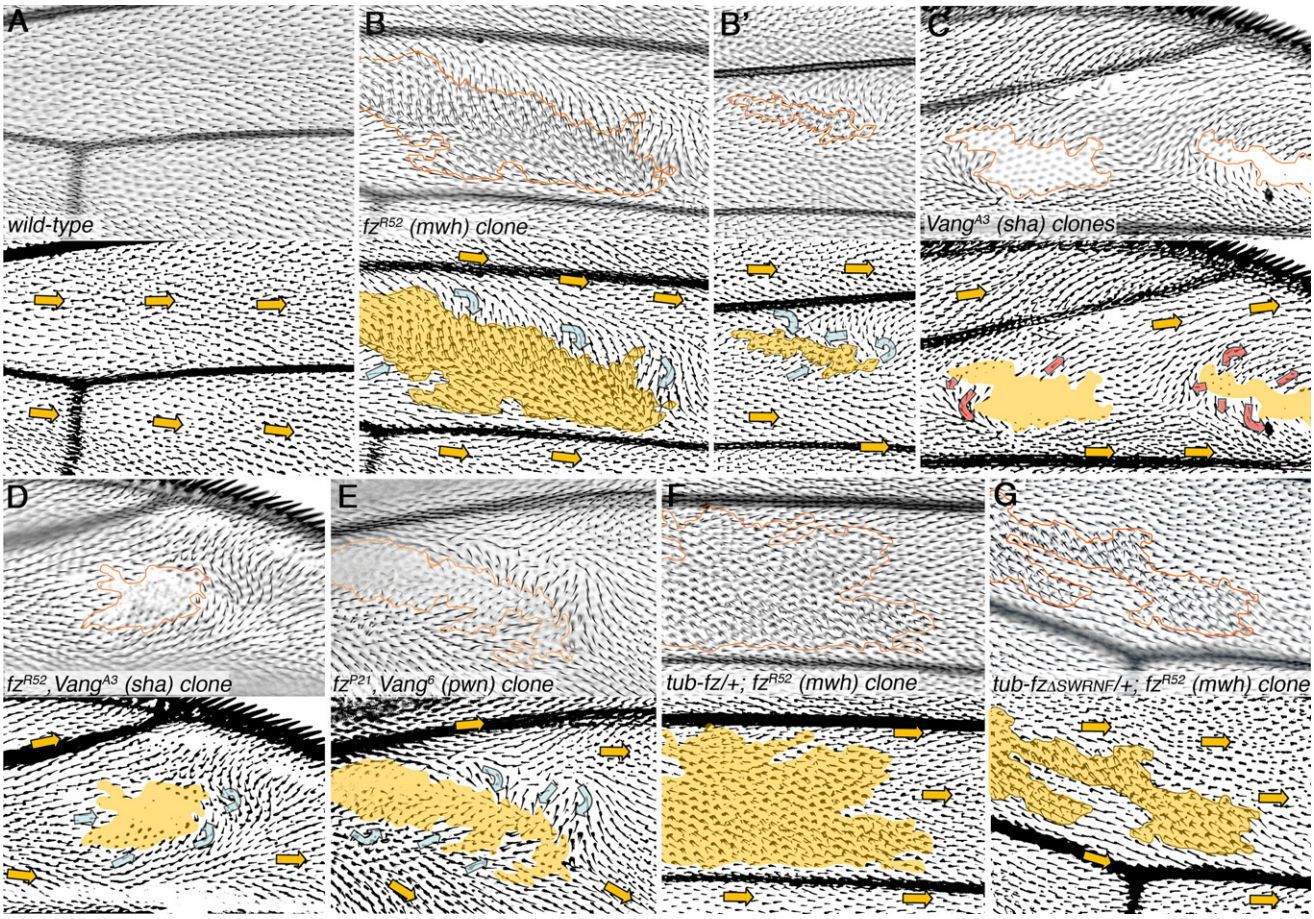

Figure 1. Nonautonomous PCP Effects of *fz* and *Vang/stbm*

All panels show high magnifications of areas of adult wings; proximal is left and anterior is up. Clones are outlined by orange lines in upper panels, and lower panels show a schematized version of the same picture (clones marked by semitransparent orange mask) and arrows indicating the cellular orientation. Yellow arrows indicate wild-type orientation, blue arrows represent areas where wing hairs orient toward mutant area, and red arrows show where cells orient away from the mutant area. The genotypes are as indicated.

(A) Wild-type.

(B and B′) Large and small fz^- (fz^{R52}) clones marked by the cell-autonomous *multiple wing hairs* (*mwh*) marker.

(C) *Vang/stbm-* ($Vang^{A3}$) clone (marked by *shavenoid/sha* [Ren et al., 2006], causing loss of cellular hairs autonomously).

(D) fz^{R52}, $Vang^{A3}$ double mutant clone (marked by *sha*).

(E) fz^{P21}, $Vang^{6}$ double mutant clone (marked by *pwn*).

All double mutant genotypes tested were generated by different means and with different transgene rescues (see Supplemental Data) and caused the same effects, largely similar to the nonautonomy associated with single mutant fz^- clones [cf. (D and E) with (B and B′)].

(F and G) Ubiquitous (*tubulin* promoter) expression of Fz and FzΔSWRNF both rescue the nonautonomous effect of fz^{R52} mutant clones [compare to (B and B′)].

RESULTS

Nonautonomous PCP Effects of *fz* and *Vang/stbm*

Wild-type cells generally re-orient toward a fz^- clone (Figures 1B and 1B′; also the Introduction and Vinson and Adler, 1987) or away from a $Vang/sbm^-$ clone (Figure 1C; Taylor et al., 1998). This raises the question of whether cells are interpreting Fz activity/levels, Vang/Stbm activity, or both during nonautonomous signaling. To address this, we generated fz^-, $Vang/stbm^-$ double mutant clones. Strikingly, wild-type cells surrounding the double mutant clones point toward the clone, just as they would do toward fz^- single mutant clones. These nonautonomous effects were observed at a very similar frequency and strength for all respective genotypes (Figures 1D and 1E, quantified in Table 1).

Recent papers have suggested that fz^-, $Vang/stbm^-$ double mutant clones display hardly any mutant defects, autonomous or nonautonomous (Strutt and Strutt, 2007; Chen et al., 2008), and thus we wished to confirm our results with different alleles and genetic backgrounds. In all double mutant genotypes with different fz^- and $Vang^-$ alleles and Fz rescue transgenes in adult and in pupal wings (Figures 1D and 1E; Table 1; Figure S1 available online; and data not shown), we always observed the same effects, with the double mutant clones behaving like fz single mutant clones in causing surrounding cells to point towards the clones (cf. Figures 1B and 1B′). Although there are rare clones resembling the one presented by Strutt and Strutt (2007), most $Vang^-$ fz^- double mutant clones display fz^- like phenotypes (see Table 1 for quantification of the nonautonomous

Table 1. Quantitative Analysis of *fz*$^{-}$ and *Vang/stbm*$^{-}$ Clone Nonautonomy

Genotype	Frequency of Effect	Orientation Relative to Clone	Clones (n)
mwh, ***fz^{R52}*** clones	85.7%	Toward	56
Vang^{A3}, *sha^{VB13}* clones	88.6%	Away	79
fz^{R52}/fz^{P21}, Vang^{A3}, *sha^{VB13}* clones (in ***tub-fz*** background)	83.6%	Toward	67
fz^{P21}, Vang^{6} *pwn* clones (in ***tub-fz*** background)	82.5%	Toward	40
fz^{P21}, Vang^{6} *pwn* clones (in ***2Xarm-fzGFP*** background)[a]	69.7%	Toward	33

General *fz* mutant phenotypes were rescued with a transgene (*tub-fz* or *2Xarm-fzGFP*) near the wild-type *Vang* locus on chromosome two. Double mutant clones were made by recombination on chromosome two, homozygosing the mutant *Vang* allele; the Fz-rescuing transgenes assorted with the wild-type allele of *Vang* and thus were lost from the *Vang* mutant clones. *fz* and *Vang* alleles and rescue constructs are in bold. The percentage of clones that exerted a nonautonomous effect on their wild-type neighbors was analyzed. The orientation of the wild-type cells showing the nonautonomous effect is indicated.

[a] The frequency of clones displaying non-autonomy is slightly lower than the other frequencies. This is likely caused by the fact that 2X*arm-fzGFP* is only able to partially rescue *fz* null mutants.

phenotypes in different genetic combinations). We further examined *Vang*$^{-}$ *fz*$^{-}$ double mutant clones with an inverse approach using a *Vang* transgene rescue (Figure S1C). This approach yielded the same nonautonomous phenotypes, with distal and lateral cells reorienting toward the mutant area, as in all other experiments with *fz*$^{-}$ or *Vang*$^{-}$ *fz*$^{-}$ clones. Our results can be reproduced with all allelic combinations and genetic backgrounds tested and they have been independently observed by others (G. Struhl, J. Casal, and P.A. Lawrence, personal communication). A recent paper by Chen et al. (2008) states that *Vang*$^{-}$*fz*$^{-}$ clones show no nonautonomous effects. However, data presented in Chen et al. (2008) may also reflect nonautonomous repolarization in wild-type cells neighboring *Vang*$^{-}$ *fz*$^{-}$ double mutant clones, as Fz protein accumulation is evident even in their experiment at the border of the clone in wild-type cells (Fz localization precedes and directs the hair orientation, thus either Fz localization or hair orientation can represent a readout of PCP signaling). Overall, we conclude that *Vang/stbm*$^{-}$, *fz*$^{-}$ double mutant clones display largely indistinguishable nonautonomous phenotypes to *fz*$^{-}$ clones, and thus that Fz levels/activity, rather than Vang/Stbm levels, play the principal role in nonautonomous contributions to the planar orientation of wing disc epithelial cells.

How do cells measure their neighbors' Fz activity (or levels)? Fz acts as a receptor and signals cell autonomously through Dsh in both Wnt-Fz/β-catenin and Fz-PCP signaling (Boutros and Mlodzik, 1999; Veeman et al., 2003; Wallingford and Habas, 2005). Therefore, Fz might signal to downstream effectors to generate a secondary signal that then acts as a relay of Fz activity to neighboring cells. However, nonautonomous Fz signaling appears to be independent of Dsh (based on analyses in *dsh* mutant backgrounds; Lee and Adler, 2002; Strutt and Strutt, 2002). To confirm this, we tested whether FzΔSWRNF (a Fz mutant that cannot interact with Dsh) (Umbhauer et al., 2000; Wong et al., 2003; Wu et al., 2008) has nonautonomous activity. Uniformly expressed *tub-fzΔSWRNF* (see Figure 2A for schematic of transgene) fully rescued the nonautonomous effects of *fz* null clones (Figure 1G; compare to rescue with wild-type *tub-fz* in Figure 1F). These data confirm that the Fz nonautonomous effect is not mediated by its Dsh-dependent intracellular signaling cascade and suggest that extracellular Fz mediates this function.

The Early Timing of Nonautonomous Fz Signaling Correlates with PCP Establishment

Since previous work has suggested that nonautonomous signaling acts earlier than autonomous signaling and thus is associated with very early events in PCP establishment (Strutt and Strutt, 2002), we tested the timing of the Fz nonautonomous function directly in a gain-of-function assay, using *dppGal4* to drive *UAS-fz* or *UAS-fzΔSWRNF* expression in a stripe along the antero-posterior compartment boundary (Figures 2B and 2C; see Figure S2 for information on the *dpp-Gal4* driver). We used the temperature-sensitive Gal4/Gal80^{ts} system to regulate the expression of these transgenes (see Figure S3 for description of assays). The animals were kept at 18°C (to repress *fz* transgene expression) and transiently shifted to 29°C (to allow expression) at different periods during pupal development. Strong nonautonomous phenotypes were only produced by temperature shifts during the 14–24 hr APF time window (summarized in Figure 2F; see Figure S3 for data and additional description). Moreover, since FzΔSWRNF (Figure 2C) performed equivalently to wild-type Fz (Figure 2B) in these assays, Dsh-dependent cell-autonomous effects of the transgene were not a factor. Indeed, late expression of Fz, during time points associated with autonomous signaling, did not exert nonautonomous PCP effects. Thus, nonautonomous functions peak at around 14–24 hr APF (Figures 2F and S3), generally preceding and partially overlapping with the beginning of robust asymmetric distribution of core PCP factors (e.g., Fz, Fmi, or Dsh; summarized in Figure 2F) (also Axelrod, 2001; Strutt, 2001; Usui et al., 1999, but see also Classen et al., 2005 for a distinct view). These results validate our assays as tools to characterize nonautonomous Fz functions during PCP establishment and confirm that early nonautonomous Fz signaling plays an instructive role.

The Fz CRD Is the Critical Protein Region in Nonautonomous Signaling

It has been shown that the cystein rich domain (CRD) is required for correct PCP establishment (Boutros et al., 2000; Chen et al., 2004). We confirmed this by showing that *tub-fzΔCRD* (see Figure 2A for schematic outline of Fz isoform) does not rescue the *fz*$^{P21/R52}$ allelic combination (Figure 2G; data not shown).

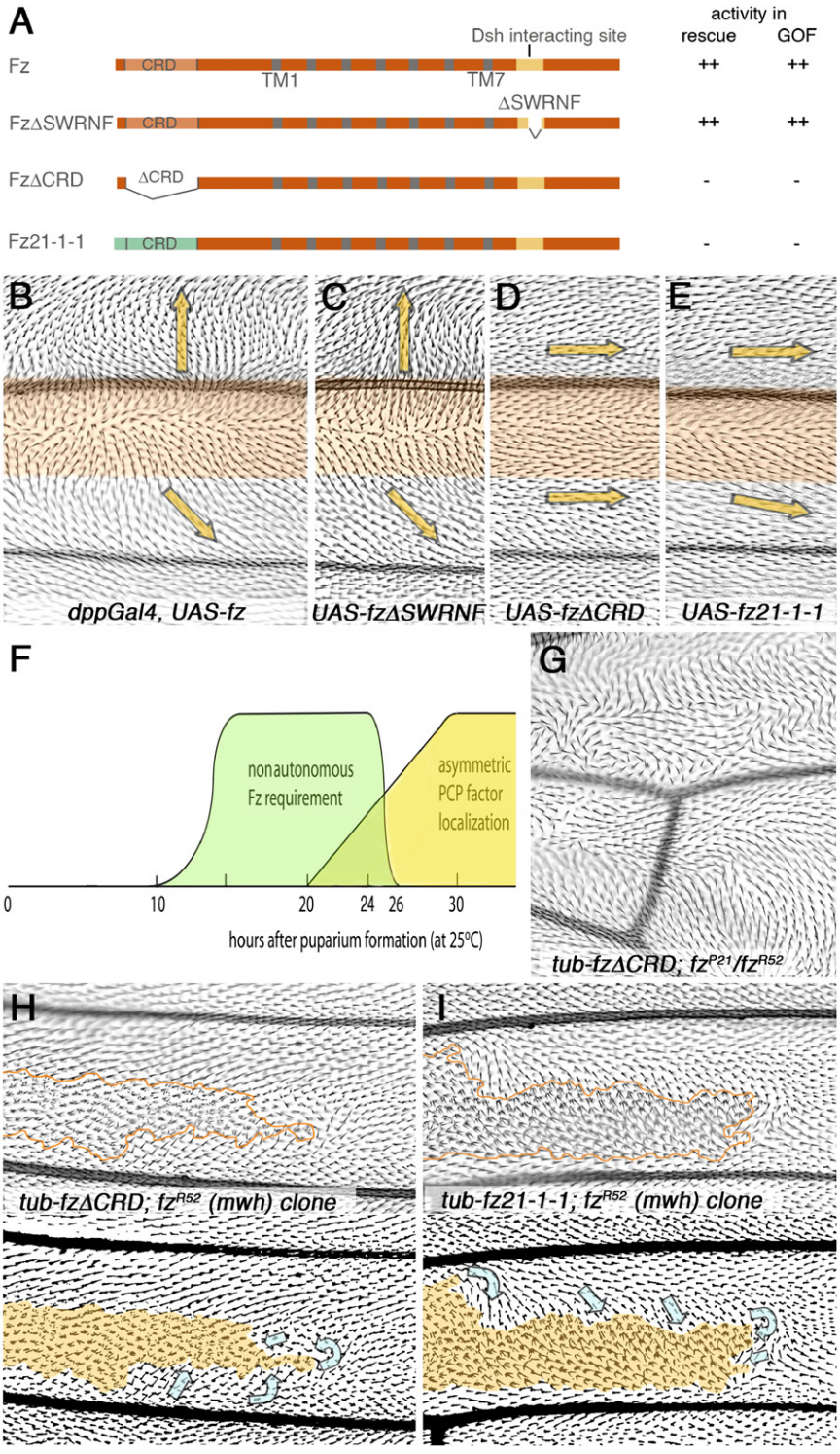

Figure 2. The Fz CRD Is Required In Vivo for Nonautonomous Signaling

(A) Schematic illustration of different mutant Fz isoforms used in this study and a summary of their nonautonomous effects in rescue and gain-of-function (GOF) assays. In the Fz/Fz2 chimera (Fz21-1-1), sequences from Fz are shown in orange, while those from Fz2 are in green. The Dsh interacting site is shown in yellow and the Fz TM domains are in gray.

(B–D) Adult wings of indicated genotypes; proximal is left and anterior is up. The respective Fz isoforms were expressed under UAS control with *dppGal4*. Approximate region of Gal4 expression is shown in orange; precise *dppGal4, UAS-GFP* expression domain is shown in Figure S2A. The resulting reorientation of neighboring cells is indicated by yellow arrows. (B) *dppGal4, UAS-fz*; (C) *dppGal4, UAS-fzΔSWRNF*; (D) *dppGal4, UAS-fzΔCRD*; (E) *dppGal4, UAS-fz21-1-1*. Deletion or replacement of the FzCRD abrogates Fz's nonautonomous activity.

(F) Schematic summary of the temporal progression of PCP events: nonautonomous signaling (as determined with the Gal4/Gal80^{ts} system; see Figure S3 for all data and experimental details) peaks between 14–24 hr APF (indicated in green); asymmetric PCP factor localization begins late during this process and is not robust until roughly 24 hr APF (in yellow).

(G–I) Rescue assays with mutant Fz isoforms affecting the CRD (adult wings oriented proximal to the left and anterior is up). (G) fz^{P21}/fz^{R52} mutant with *tub-fzΔCRD*. PCP defects remain without an apparent rescue of the mutant phenotype (the defective polarity pattern is however different from fz^{P21}/fz^{R52} wings) (Wu et al., 2008). (H and I): Rescue assay of fz^{-} clonal phenotype. Clones are marked by *mwh* and highlighted by orange outline; lower panels show stylized presentation of same wing area, clone mask and arrows are as in Figure 1. Ubiquitous (*tubulin* promoter) expression of FzΔCRD (H) or Fz21-1-1 [(I); see (A) for schematic of isoforms] does not rescue nonautonomous effects associated with fz^{-} clones (compare to wild-type Fz in Figure 1F).

All other functional aspects of Fz were indistinguishable between wild-type Fz and FzΔCRD: it was stably expressed, localized to the subapical cellular membrane domain, recruited Dsh to the membrane like wild-type Fz (Figure S4A), and importantly it rescued the canonical Wg-signaling function of Fz (Figure S4B), which does not require the CRD (Chen et al., 2004).

To address whether the CRD is important for nonautonomous signaling, we first tested FzΔCRD in the *dppGal4* based gain-of-function assay described above. In contrast to wild-type Fz or FzΔSWRNF, FzΔCRD failed to reorient cellular polarity, and wing hairs remained oriented in the proximo-distal axis (Figure 2D, compare to *wt* Fz in Figure 2B). Similarly, a swap of the FzCRD for the Fz2CRD (Fz21-1-1, see Figure 2A for schematic outline) eliminated the nonautonomous activity of the transgene (Figure 2E). Taken together, these data suggested that the Fz CRD is the critical and active part in Fz, mediating its nonautonomous signaling activity. In fact, fz^{-} clones continue to exert domineering nonautonomy (reorienting wild-type neighbors)

even when they express FzΔCRD (*tub-fzΔCRD*; Figure 2H, cf. Figures 1B and 1B′; 92.3% of clones had surrounding wild-type cells pointing toward clone, n = 39) or the chimeric protein containing the Fz2CRD (*tub-fz21-1-1*, Figure 2A for schematic, Figure 2I for result). Taken together, these experiments indicate that the Fz CRD is a critical domain required for nonautonomous Fz/PCP signaling in vivo.

The Fz Extracellular Domain (ECD) Can Bind to Vang/Stbm

Since Vang is not required in Fz-expressing cells for them to exert a nonautonomous effect but is required in the responding tissue for the downstream cell-autonomous transduction of that effect (Lawrence et al., 2004; Taylor et al., 1998), we considered the possibility that Vang is a Fz receptor.

We thus tested whether the Fz ECD sequences and Vang/Stbm can physically interact. First, we fused the FzECD to human placenta alkaline phosphatase (AP), and employed the fusion protein in a cell-free pulldown assay. FzECD-AP was bound to anti-AP beads; a cell lysate from YFP-tagged Vang/Stbm (YFP-Vang) expressing cells (see Experimental Procedures) was passed over the FzECD-AP beads and control AP beads (see Figure 3A for a schematic outline). Whereas FzECD-AP pulled down YFP-Vang/Stbm, the control AP did not (Figure 3B). To confirm the specificity of this binding, we tested the ECD of Smoothened (Smo, a protein related to Fz which also harbors a CRD-like sequence; SmoECD-AP) and the ECD of CDO (a mouse protein that binds Shh and acts in the Smo pathway) (Tenzen et al., 2006). Whereas YFP-Vang bound to FzECD, it did not interact with SmoECD-AP or CDO-AP (Figure 3C, left panel). In a second assay, we tested for binding of the secreted FzECD-AP protein to YFP-Vang expressing cells (Figure 3D). The binding can be assayed by AP activity associated with the respective YFP-Vang expressing cells (see Experimental Procedures). Similarly to the in vitro assay, FzECD-AP showed significant binding to YFP-Vang expressing cells (Figure 3D). To test for specificity from the Vang/Stbm side, we expressed a different tetra-span TM protein (YFP-CD9), as well as a form of Vang that carried point mutations in its extracellular loops (YFP-Vang^{mut}; see Figure S5 for details). FzECD-AP bound to neither YFP-Vang^{mut} nor YFP-CD9 expressing cells (Figure 3E). Taken together, these data indicated that the FzECD specifically interacted with Vang/Stbm.

As the CRD is critical in in vivo assays (Figure 2), we next tested whether the CRD sequences are sufficient for the physical interaction with Vang/Stbm in vitro. Whereas FzECDΔCRD-AP did not pull down YFP-Vang (Figure 3C, right panel), FzCRD-AP by itself bound to YFP-Vang efficiently, although to a slightly lesser extent than full-length FzECD (Figure 3C, right panel). These data indicated that the CRD is the critical domain within the extracellular region of Fz for its physical binding to Vang/Stbm.

DISCUSSION

Our data suggest that the Fz ECD, including the CRD, acts as a Vang/Stbm ligand in nonautonomous signaling (see model, Figures 3F and 3G). How do these data and interpretations fit with other existing results and models?

The FzECD, in Particular the CRD, Are Essential for PCP Function

The Fz CRD is clearly dispensable for canonical Wg signaling in vivo (Chen et al., 2004). Previous studies have shown that it is essential for PCP signaling (Boutros et al., 2000; Chen et al., 2004; Strapps and Tomlinson, 2001); however, the specifics of when and where have been controversial. A recent paper suggests that the CRD is not strictly required for PCP establishment (Chen et al., 2008), as FzΔCRD can partially rescue *fz* mutant phenotypes in the wing. However, some PCP defects remain. It is also worth noting that in experiments where Chen et al. (2008) assay the multiple wing hair phenotype of *fz* wings, this serves as a marker for late stage cell-autonomous Fz functions (Krasnow and Adler, 1994) and does not address whether FzΔCRD is functional in intercellular nonautonomous communication. Our experiments indicate that FzΔCRD does not fully rescue *fz* PCP phenotypes and does not affect domineering nonautonomy of *fz* mutant clones (Figure 2). Thus, we conclude that the CRD of Fz is necessary for cells to send polarizing signals to neighboring cells.

The Role of Fz and Vang/Stbm in Nonautonomous PCP Signaling

Genetic (Figure 1) and physical (Figure 3) interaction data suggest that at the early PCP signaling stage (14–24 hr APF; Figure 2F), Vang/Stbm functions as a receptor for FzCRD. As such, it would appear that Vang/Stbm senses how much Fz (activity) is present on adjacent cells and relays this information, causing a cell to orient toward the neighboring cell with lower Fz level/activity (see model in Figures 3F and 3G). Our conclusion that Fz "signals" and Vang "receives the signal" is consistent with previous models by Lawrence et al. (2004), in that a *fz*$^{-}$ cell at the clone boundary will orient toward the center of the mutant area as it compares levels of its two neighboring cells (one of which is the wild-type cell adjacent to the clone). Similarly, it has been shown that *Vang* is not needed in the "sending" cell (Lawrence et al., 2004), which is consistent with the result that *fz*$^{-}$ *Vang*$^{-}$ double mutant clones behave like *fz*$^{-}$ clones. How do these observations fit with the nonautonomous behavior of *Vang*$^{-}$ clones? In *Vang*$^{-}$ mutant cells, all Fz protein accumulates at the membranes abutting wild-type cells; wild-type cells at the clonal border would therefore presumably detect more Fz in *Vang*$^{-}$ cells. Our model would predict that this relocalization of Fz causes these cells to orient away from the *Vang*$^{-}$ neighbors. This interpretation is also consistent with the *Vang*$^{-}$ phenotype being suppressed in *fz*$^{-}$ *Vang*$^{-}$ double mutant clones, suggesting that the nonautonomous effect is mediated largely through Fz.

Fz-Vang/Stbm interactions are dependent on the presence of the Fmi (also known as Stan) protein (Lawrence et al., 2004; Casal et al., 2006) but are independent of the core PCP factor Dsh (Figure 1G; also Lee and Adler, 2002; Strutt and Strutt, 2002). Similarly, they are independent of Pk, which mediates the cell-autonomous requirement for Vang/Stbm (Bastock et al., 2003; Jenny et al., 2003). It is important to note that *Vang/stbm* mutants affect *fz*$^{-}$ nonautonomy differently from *pk* mutants: *Vang/stbm*$^{-}$ backgrounds suppress the domineering nonautonomy of *fz*$^{-}$ clones (consistent with our model), whereas *pk*$^{-}$ mutants enhance the nonautonomous effects (Adler et al.,

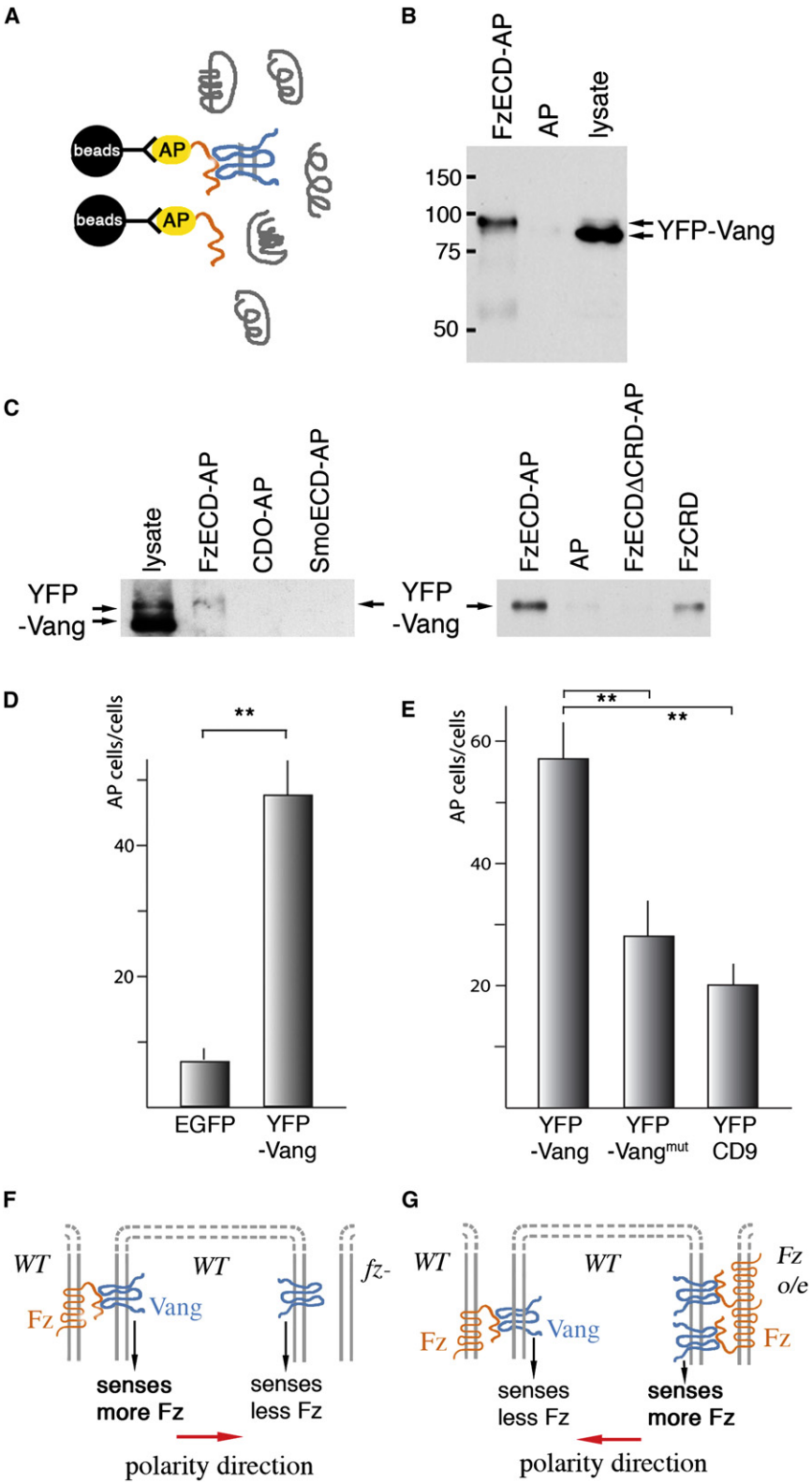

Figure 3. Direct Physical Association of the Fz CRD with Vang/Stbm

(A) Schematic presentation of the pull-down assay involving the FzECD fused to AP (alkaline phosphatase), anti-AP beads (black), and YFP-Vang/Stbm-containing cell extracts. Yellow, AP; orange, FzECD; blue, YFP-Vang; gray, any protein.

(B and C) Western blots (anti-YFP) of eluates from anti-AP agarose beads absorbed with 0.8 pmol proteins as indicated over which a lysate of YFP-Vang expressing cells was passed. (B) From left: FzECD-AP, control AP, and the lysate itself. In the lysate, YFP-Vang appears as two bands with the slower migrating band being less abundant (possibly a mature fully processed form). The slower migrating band is preferentially bound by FzECD. (C) Specificity controls for binding. Left blot (from left): total lysate, FzECD-AP, CDO-AP, SmoECD-AP. Right blot (from left): FzECD-AP, AP, FzECDΔCRD-AP, FzCRD. The FzCRD binds specifically and is sufficient for binding to YFP-Vang.

(D and E) Cell binding assay. Fraction of transfected (YFP–positive) cells that also bound FzECD-AP as compared to control cells (EGFP) is presented as AP cells (YFP/AP double-positive)/cells (average of three independent experiments with SD). (E) Specificity controls with Vang^{mut}, which carries three point mutations in its extracellular loops (see Figure S5), and CD9, an unrelated tetraspan transmembrane protein. YFP-Vang-expressing cells bind significantly more FzECD-AP (p values of < 0.005 indicated by **). AP alone does not bind any of these cell types (data not shown).

(F and G) Schematic illustrations of how Fz levels are sensed by Vang/Stbm in wild-type (WT) cells abutting mutant (*fz*$^{-}$ or Fz overexpressing[o/e]) clones. In wild-type tissues, the generation of a Fz "activity" gradient must be mediated by other factors that modify Fz, Vang/Stbm, or their interaction in a graded manner (see main text).

Vang/Stbm interactions: the nonautonomous phase addressed here (14–24 hr APF; Figure 2) and a later autonomous phase involving Dsh and Pk (as proposed by Amonlirdviman et al., 2005).

Fz-Vang As Compared to Fmi-Fmi Interactions

The simplest interpretation of our data suggests signaling from Fz to Vang/Stbm during nonautonomous signaling (Figure 3). We cannot exclude, however, that the interaction is bidirectional and that Fz activity is also influenced by binding to Vang/Stbm (in a Dsh-independent manner). Nevertheless, comparing the gain-of-function data of Fz and Vang/Stbm, the effects of Fz in repolarizing neighboring cells are always robust (e.g., Figures 2B and 2C), whereas those with Vang/Stbm are milder and

2000). These data suggest that during early nonautonomous PCP signaling, Fz-Vang/Stbm effects are independent of Pk. It is thus likely that there are two distinguishable phases of Fz-

more cell autonomous (Figure S6 and Darken et al., 2002). Despite this observation, bidirectional signaling is possible, either through the Fz-Vang/Stbm interaction or through their links to the atypical cadherin Fmi as suggested in several models (Lawrence et al., 2004; Klein and Mlodzik, 2005; Casal et al., 2006; Le Garrec et al., 2006). Our data do not exclude an instructive role for a Fmi-Fmi interaction as proposed earlier (Klein and Mlodzik, 2005; Casal et al., 2006; Le Garrec et al., 2006; Chen et al., 2008). Indeed, this latter idea is supported by the observation that nonautonomous *fz*$^-$ clonal phenotypes are not completely suppressed in a *Vang*$^-$ mutant background, as some nonautonomy is still observed (~25% of *fz*$^-$ clones still display weak nonautonomy in a *Vang*$^-$ background; Taylor et al., 1998).

Fmi has recently been shown to associate with Fz (Chen et al., 2008), and thus the homophilic cell adhesion behavior of Fmi could also contribute to an instructive directional signal. The observations that Fz can associate extracellularly with Vang/Stbm (this work) and within the membrane with Fmi (Chen et al., 2008) suggest a complex scenario. A cross-cell interaction mediated by the homophilic Fmi interaction could display asymmetric properties, as Fmi-Fz and/or Fmi-Vang complexes could have different qualities and signal in either direction (Klein and Mlodzik, 2005; Casal et al., 2006; Le Garrec et al., 2006). However, *fmi* null clones show little nonautonomous behavior (a 1 cell wide effect) (Lawrence et al., 2004; Casal et al., 2006), while the *fz*$^-$ and *fz*$^-$ *Vang*$^-$ clones with widespread nonautonomy are nevertheless striking. Fmi causes significant nonautonomy when overexpressed, and this effect seems not to depend on the presence of Fz or Vang in the overexpressing clone (Chen et al., 2008). Multiple parallel mechanisms are thus likely to exist that contribute to cell-cell communication in transmitting the polarity signal.

In conclusion, we provide here molecular evidence for a mechanism of nonautonomous Fz signaling through direct interactions with Vang/Stbm on neighboring cells. It remains unclear how the levels of the initial Fz-Vang/Stbm interaction are established in wild-type. Both Fz and Vang/Stbm are expressed evenly and their initial subcellular localization is not polarized. Thus, in wild-type, the generation of a polarized Fz-Vang/Stbm interaction (across cells) must be mediated by other factors that modify Fz, Vang/Stbm, or their interaction in a graded manner.

EXPERIMENTAL PROCEDURES

Fly Strains and Genetics

Generation of double mutant *fz*$^-$, *Vang*$^-$ clones: as *fz* and *Vang* are not on the same chromosome, we used a *tub-fz* (*tubulin* promoter driven Fz expression) on the second chromosome (2R) to rescue *fz*$^-$ phenotypes. When *Vang*$^-$ clones (labeled with *sha*$^-$, with no or very short wing hairs) (Ren et al., 2006) are induced in *fz*$^-$, *tub-fz* background, *tub-fz* rescue is lost in *Vang/stbm*$^-$ clones, and such clones lack both Vang/Stbm and Fz proteins. *Vang*^{A3} (genetic null allele), *Vang*^{6} (protein null allele), *fz*^{P21} (null), and *fz*^{R52} (strong allele) were used (Jones et al., 1996; Taylor et al., 1998; Wolff and Rubin, 1998). *FRT42 pwn Vang*^{6} was obtained from Gary Struhl. *arm-fz-GFP* is as described (Strutt and Strutt, 2007). Detailed genotypes of the respective flies are shown in Supplemental Data.

Fz constructs were Myc tagged (Boutros et al., 2000); FzΔSWRNF (= Fz1-1-1ΔSWRNF) and Fz21-1-1 (= Fz2-1-1) were as described (Boutros et al., 2000; Wu et al., 2004, 2008). FzΔCRD was generated by introducing HindIII sites after residues N51 and E166, and amino acids between N51-E166 were thus deleted. PCR-based mutagenesis was used to generate all mutant Fz isoforms (Quikchange kit, Stratagene). SmoECD-AP was constructed by cloning corresponding to residues 1–219 into the HindIII site of AP teg2 vecor. Rabbit anti-Fz was a gift from David Strutt (Bastock and Strutt, 2007). Immunohistochemistry and wing preparation were performed as in Wu et al. (2004).

Molecular Interactions

AP fusion proteins were produced in HK293T cells, and their activity was used to quantify the amount of AP proteins used (Flanagan et al., 2000). Cells were lysed 3 days later in 50 mM Tris (pH 7.5), 150 mM NaCL, 1 mM EDTA with 0.5% Triton X-100 and protease inhibitors (from Sigma) to prepare YFP-Vang lysate.

Direct Binding Assay

Cell culture media containing 0.8 pmol FzECD-AP, AP, FzECDΔCRD-AP, or FzCRD-AP were incubated with 30 μl anti-AP agarose beads (Sigma; based on AP activity assay, over 99% of each fusion protein was absorbed onto beads). The bead samples were incubated with equal amounts of YFP-Vang lysate (cell membranes were dissolved by detergent in the lysate; the same preparation was used for the different AP-fusion beads) for 2 hr at 4°C, washed 4–5× with 50 mM Tris (pH 7.5), 150 mM NaCL, 0.1% Triton X-100, and bound proteins eluted and analyzed by western blotting (mouse anti-GFP, Roche).

Cell Binding Assays

Cos7 cells were transfected with control EGFP alongside either YFP-Vang pCS2 (from A. Jenny), YFP-Vang mutant, or YFP-CD9 (an unrelated tetraspanin). The AP binding assay was modified from Flanagan et al. (2000). COS7 cells seeded in 12-well plates at 20%–30% confluence were transfected with 0.2–0.4 μg DNA each. Three days after transfection, 0.02–0.08 nM FzECDAP or AP supernatant (buffered in 10 mM or 20 mM HEPES pH 7.0) was added and incubated for 2 hr at room temperature. Cells were washed 6 times (5 min each) with HBHA buffer (GenHunter). Samples were fixed in 2% formaldehyde HBS for 5 min and washed twice with HBS. Plates were first incubated at 65°C for 45–60 min to inactivate endogenous AP, then incubated for 5 min with AP buffer and subsequently stained with AP staining solution (Zymed AP staining kit, Invitrogen) to reveal AP fusion protein stain.

SUPPLEMENTAL DATA

Supplemental Data include six figures, Supplemental Experimental Procedures, and Supplemental References and can be found with this article online at http://www.developmentalcell.com/cgi/content/full/15/3/462/DC1/.

ACKNOWLEDGMENTS

We thank Paul Adler, David Strutt, Stephen Cohen, Jeffrey Axelrod, and Jessica Treisman for flies and plasmids and Jong-Sun Kang and Robert Krauss for advice and tools for the physical binding studies. We are most grateful to Gary Struhl for sharing unpublished results, many fly strains, and helpful comments and to Yanfeng Wang for the gift of an unpublished fly strain. We acknowledge the help of Z. Du and S. Okello for help with generating transgenic flies. We thank Peter Lawrence for helpful discussions and D. del Alamo, R. Krauss, T.J. Klein, J. Seifert, and U. Weber for comments on the manuscript. This work was supported by NIH/NIGMS grant RO1GM62917 to MM.

Received: January 31, 2008
Revised: June 25, 2008
Accepted: August 18, 2008
Published: September 15, 2008

REFERENCES

Adler, P.N. (2002). Planar signaling and morphogenesis in *Drosophila*. Dev. Cell *2*, 525–535.

Adler, P.N., Krasnow, R.E., and Liu, J. (1997). Tissue polarity points from cells that have higher Frizzled levels towards cells that have lower Frizzled levels. Curr. Biol. *7*, 940–949.

Adler, P.N., Taylor, J., and Charlton, J. (2000). The domineering non-autonomy of *frizzled* and *van Gogh* clones in the *Drosophila* wing is a consequence of a disruption in local signaling. Mech. Dev. *96*, 197–207.

Amonlirdviman, K., Khare, N.A., Tree, D.R., Chen, W.S., Axelrod, J.D., and Tomlin, C.J. (2005). Mathematical modeling of planar cell polarity to understand domineering nonautonomy. Science *307*, 423–426.

Axelrod, J.D. (2001). Unipolar membrane association of Dishevelled mediates Frizzled planar cell polarity signaling. Genes Dev. *15*, 1182–1187.

Bastock, R., and Strutt, D. (2007). The planar polarity pathway promotes coordinated cell migration during Drosophila oogenesis. Development *134*, 3055–3064.

Bastock, R., Strutt, H., and Strutt, D. (2003). Strabismus is asymmetrically localised and binds to Prickle and Dishevelled during Drosophila planar polarity patterning. Development *130*, 3007–3014.

Boutros, M., and Mlodzik, M. (1999). Dishevelled: at the crossroads of divergent intracellular signaling pathways. Mech. Dev. *83*, 27–37.

Boutros, M., Mihaly, J., Bouwmeester, T., and Mlodzik, M. (2000). Signaling specificity by Frizzled receptors in *Drosophila*. Science *288*, 1825–1828.

Casal, J., Lawrence, P.A., and Struhl, G. (2006). Two separate molecular systems, Dachsous/Fat and Starry night/Frizzled, act independently to confer planar cell polarity. Development *133*, 4561–4572.

Chen, C.M., Strapps, W., Tomlinson, A., and Struhl, G. (2004). Evidence that the cysteine-rich domain of Drosophila Frizzled family receptors is dispensable for transducing Wingless. Proc. Natl. Acad. Sci. USA *101*, 15961–15966.

Chen, W.S., Antic, D., Matis, M., Logan, C.Y., Povelones, M., Anderson, G.A., Nusse, R., and Axelrod, J.D. (2008). Asymmetric homotypic interactions of the atypical cadherin flamingo mediate intercellular polarity signaling. Cell *133*, 1093–1105.

Classen, A.K., Anderson, K.I., Marois, E., and Eaton, S. (2005). Hexagonal packing of Drosophila wing epithelial cells by the planar cell polarity pathway. Dev. Cell *9*, 805–817.

Darken, R.S., Scola, A.M., Rakeman, A.S., Das, G., Mlodzik, M., and Wilson, P.A. (2002). The planar polarity gene strabismus regulates convergent extension movements in Xenopus. EMBO J. *21*, 976–985.

Fanto, M., and McNeill, H. (2004). Planar polarity from flies to vertebrates. J. Cell Sci. *117*, 527–533.

Flanagan, J.G., Cheng, H.J., Feldheim, D.A., Hattori, M., Lu, Q., and Vanderhaeghen, P. (2000). Alkaline phosphatase fusions of ligands or receptors as in situ probes for staining of cells, tissues, and embryos. Methods Enzymol. *327*, 19–35.

Guo, N., Hawkins, C., and Nathans, J. (2004). Frizzled6 controls hair patterning in mice. Proc. Natl. Acad. Sci. USA *101*, 9277–9281.

Jenny, A., Darken, R.S., Wilson, P.A., and Mlodzik, M. (2003). Prickle and Strabismus form a functional complex to generate a correct axis during planar cell polarity signaling. EMBO J. *22*, 4409–4420.

Jones, K.H., Liu, J., and Adler, P.N. (1996). Molecular analysis of EMS-induced *frizzled* mutations in *Drosophila melanogaster*. Genetics *142*, 205–215.

Keller, R. (2002). Shaping the vertebrate body plan by polarized embryonic cell movements. Science *298*, 1950–1954.

Klein, T.J., and Mlodzik, M. (2005). Planar cell polarization: an emerging model points in the right direction. Annu. Rev. Cell Dev. Biol. *21*, 155–176.

Krasnow, R.E., and Adler, P.N. (1994). A single Frizzled protein has a dual function in tissue polarity. Development *120*, 1883–1893.

Lawrence, P.A., Casal, J., and Struhl, G. (2004). Cell interactions and planar polarity in the abdominal epidermis of Drosophila. Development *131*, 4651–4664.

Lawrence, P.A., Struhl, G., and Casal, J. (2007). Planar cell polarity: one or two pathways? Nat. Rev. Genet. *8*, 555–563.

Le Garrec, J.F., Lopez, P., and Kerszberg, M. (2006). Establishment and maintenance of planar epithelial cell polarity by asymmetric cadherin bridges: a computer model. Dev. Dyn. *235*, 235–246.

Lee, H., and Adler, P.N. (2002). The function of the frizzled pathway in the Drosophila wing is dependent on inturned and fuzzy. Genetics *160*, 1535–1547.

Mlodzik, M. (2002). Planar cell polarization: do the same mechanisms regulate *Drosophila* tissue polarity and vertebrate gastrulation? Trends Genet. *18*, 564–571.

Montcouquiol, M., Crenshaw, E.B., 3rd, and Kelley, M.W. (2006). Noncanonical Wnt signaling and neural polarity. Annu. Rev. Neurosci. *29*, 363–386.

Ren, N., He, B., Stone, D., Kirakodu, S., and Adler, P.N. (2006). The shavenoid gene of Drosophila encodes a novel actin cytoskeleton interacting protein that promotes wing hair morphogenesis. Genetics *172*, 1643–1653.

Seifert, J.R., and Mlodzik, M. (2007). Frizzled/PCP signalling: a conserved mechanism regulating cell polarity and directed motility. Nat. Rev. Genet. *8*, 126–138.

Strapps, W.R., and Tomlinson, A. (2001). Transducing properties of *Drosophila* Frizzled proteins. Development *128*, 4829–4835.

Strutt, D.I. (2001). Asymmetric localization of frizzled and the establishment of cell polarity in the *Drosophila* wing. Mol. Cell *7*, 367–375.

Strutt, H., and Strutt, D. (2002). Nonautonomous planar polarity patterning in *Drosophila*: *dishevelled*-independent functions of *frizzled*. Dev. Cell *3*, 851–863.

Strutt, D., and Strutt, H. (2007). Differential activities of the core planar polarity proteins during Drosophila wing patterning. Dev. Biol. *302*, 181–194.

Tada, M. (2005). Notochord morphogenesis: a prickly subject for ascidians. Curr. Biol. *15*, R14–R16.

Taylor, J., Abramova, N., Charlton, J., and Adler, P.N. (1998). *Van Gogh*: a new *Drosophila* tissue polarity gene. Genetics *150*, 199–210.

Tenzen, T., Allen, B.L., Cole, F., Kang, J.S., Krauss, R.S., and McMahon, A.P. (2006). The cell surface membrane proteins Cdo and Boc are components and targets of the Hedgehog signaling pathway and feedback network in mice. Dev. Cell *10*, 647–656.

Umbhauer, M., Djiane, A., Goisset, C., Penzo-Mendez, A., Riou, J.F., Boucaut, J.C., and Shi, D.L. (2000). The C-terminal cytoplasmic Lys-thr-X-X-X-Trp motif in frizzled receptors mediates Wnt/beta-catenin signalling. EMBO J. *19*, 4944–4954.

Usui, T., Shima, Y., Shimada, Y., Hirano, S., Burgess, R.W., Schwarz, T.L., Takeichi, M., and Uemura, T. (1999). Flamingo, a seven-pass transmembrane cadherin, regulates planar cell polarity under the control of Frizzled. Cell *98*, 585–595.

Veeman, M.T., Axelrod, J.D., and Moon, R.T. (2003). A second canon. Functions and mechanisms of beta-catenin-independent Wnt signaling. Dev. Cell *5*, 367–377.

Vinson, C.R., and Adler, P.N. (1987). Directional non-cell autonomy and the transmission of polarity information by the *frizzled* gene of *Drosophila*. Nature *329*, 549–551.

Wallingford, J.B., and Habas, R. (2005). The developmental biology of Dishevelled: an enigmatic protein governing cell fate and cell polarity. Development *132*, 4421–4436.

Wang, Y., and Nathans, J. (2007). Tissue/planar cell polarity in vertebrates: new insights and new questions. Development *134*, 647–658.

Wolff, T., and Rubin, G.M. (1998). *strabismus*, a novel gene that regulates tissue polarity and cell fate decisions in *Drosophila*. Development *125*, 1149–1159.

Wong, H.C., Bourdelas, A., Krauss, A., Lee, H.J., Shao, Y., Wu, D., Mlodzik, M., Shi, D.L., and Zheng, J. (2003). Direct binding of the PDZ domain of Dishevelled to a conserved internal sequence in the C-terminal region of Frizzled. Mol. Cell *12*, 1251–1260.

Wu, J., Klein, T.J., and Mlodzik, M. (2004). Subcellular localization of frizzled receptors, mediated by their cytoplasmic tails, regulates signaling pathway specificity. PLoS Biol. *2*, E158.

Wu, J., Jenny, A., Mirkovic, I., and Mlodzik, M. (2008). Frizzled-Dishevelled signaling specificity outcome can be modulated by Diego in Drosophila. Mech. Dev., in press.

Zallen, J.A. (2007). Planar polarity and tissue morphogenesis. Cell *129*, 1051–1063.